Supplement of Atmos. Chem. Phys., 23, 7057–7074, 2023
https://doi.org/10.5194/acp-23-7057-2023-supplement

Atmospheric Chemistry and Physics
Open Access
EGU

Supplement of

OH measurements in the coastal atmosphere of South China: possible missing OH sinks in aged air masses

Zhouxing Zou et al.

Correspondence to: Tao Wang (tao.wang@polyu.edu.hk)

Supplementary Information

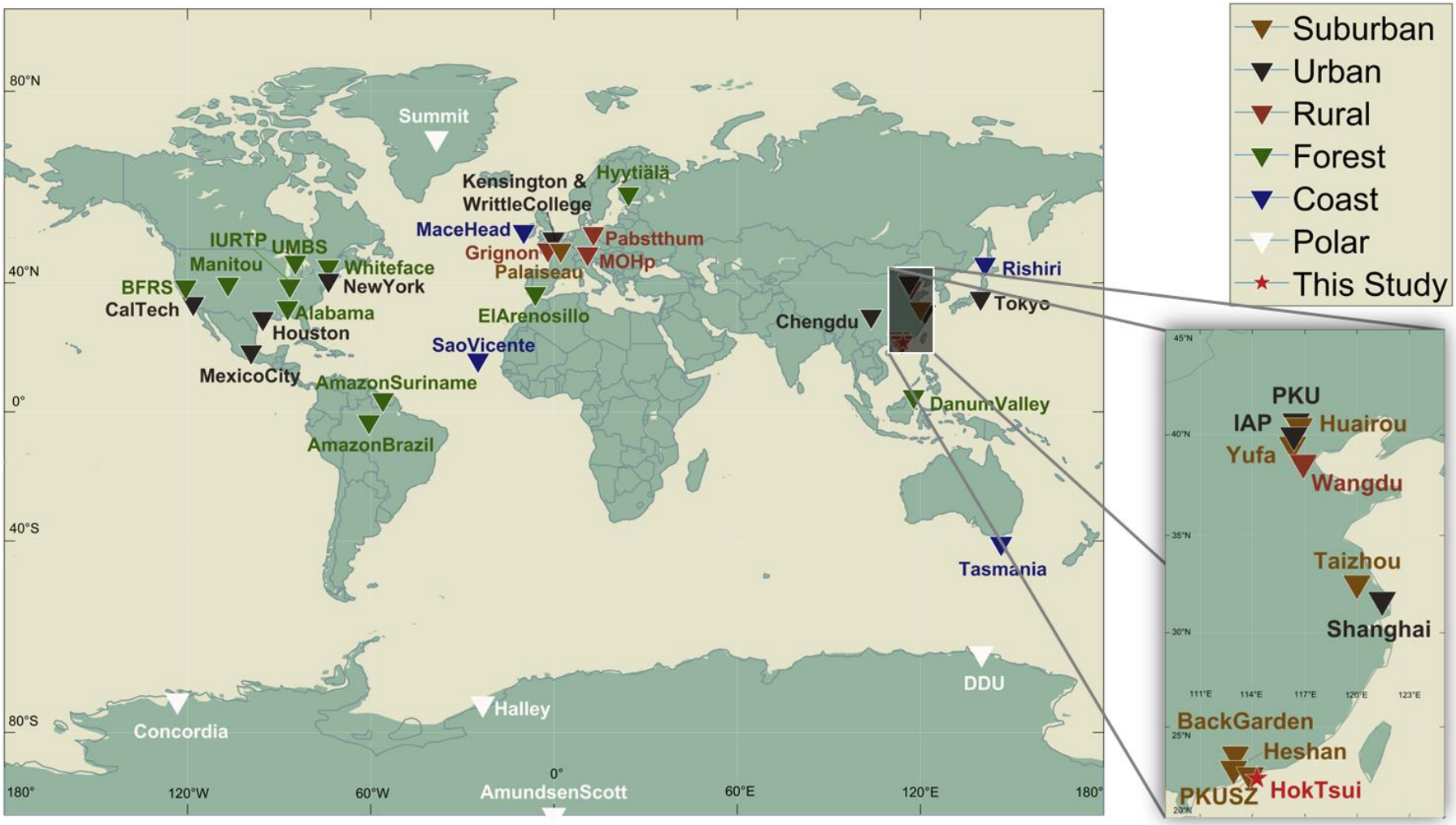

Figure S1. OH measurements gathered around the world to date.

Table S1. Summary of studies reporting OH and HO_2 measurements and comparing them with model predictions (refer to Figure S1 for site locations)

Comparison results (OH only)	Reference	Time	Location in Figure 1	Site types	Measurement notes	OH conc. 10^6 cm^{-3}	HO_2 conc. 10^8 cm^{-3}	Ratio notes	OH $R_{S/O}$	HO_2 $R_{S/O}$	Other references targeting the same site
Overprediction	Berresheim et al., 2002	June–July 1999	MaceHead	Coast	Mean (All) Peaks (Mean Clean) Peaks (Pollution)	0.12 2.5 18 & 12	N/A	Mean (17 June, Coastal) Mean (30 July, Continental)	2 ~1	N/A	Carslaw et al., 1999; Berresheim et al., 2013, 2014;
Overprediction	Sommariva et al., 2004; Creasey et al., 2003;	Jan–Feb 1999	Tasmania	Coast	Mean (Peaks) Peaks (Range)	3.5 2 to 5.5	2 1 to 2.5	Mean (7–8 Feb) Mean (15–16 Feb)	~1.11 ~1.32	N/A ~2	N/A
Overprediction	Kanaya et al., 2007	September 2003	Rishiri	Island Coast	Peaks (Mean)	2.7	1.45	OH rectified by constrained HO_2	1.35	1.89	N/A
Overprediction	Mauldin III et al., 2010	Nov–Jan 2003-04	AmundsenScott	Antarctica	Mean (Range)	1.5 to 2.5	N/A	Mean	~2	N/A	Mauldin III et al., 2001
Overprediction	Kukui et al., 2014	Dec–Jan 2011-2012	Concordia	Antarctica	Mean (All) Peaks (Mean) Mean (range)	3.1 5.2 0.3 to 7.5	0.99* 1.7* 0.1 to 2*	Mean (w/PSS HONO) Mean (w/measured HONO)	0.72 2.19	1.02* 1.84*	N/A
Overprediction	Dusanter et al., 2009a, b;	March 2006	MexicoCity	Urban	Peaks (Range) Peaks (Mean)	2 to 15 4.6	0.56 to 4.5 1.9	Mean (13:00 w/o glyoxal) Mean (Morning, polluted) Mean (11:00–14:30) Mean (After 14:30)	2.4 ~0.5 to ~1 1.7 ~1	1.5 0.2 to ~1 ~1 ~1	N/A
Overprediction	Bloss et al., 2007	Jan–Feb 2005	Halley	Polar	Mean (All) Peak (Mean)	0.39 0.79	2.04 4.03	Peak (S1: Conventional) Peak (S2: S1 + halogen oxides) Peak (S3: S2 + possible VOCs)	0.67 1.64 1.27	N/A	N/A
Overprediction	Holland et al., 2003	Jul–Aug 1998	Pabstthum	Rural	Peaks (Range)	6 to 8	5 to 7.4	Mean (Low NO_x)	2	1.4	N/A
Overprediction	Whalley et al., 2018	Jul–Aug 2012	Kensington	Urban	Mean (Noon; S-W air) Mean (Noon; E, polluted air)	~2.2 ~3	~0.2 ~0.5	Mean (Air mass: South-westerly) Mean (Air mass: Easterly, polluted)	1.25 2	~4 10	N/A
Overprediction	Griffith et al., 2016	May–June 2010	CalNexLA	Urban	Peaks (Range) Peaks (Weekdays) Peaks (Weekend)	1.5 to 9 ~4 ~5	0.8* to 10* ~3* ~8*	Mean (Weekend) Mean (Weekday)	1.43 1	0.77* 0.33*	Volz-Thomas et al., 2003b, a

Table S1. Continued

Comparison results (OH only)	Reference	Time	Location in Figure 1	Site types	Measurement notes	OH conc. 10^6 cm^{-3}	HO_2 conc. 10^8 cm^{-3}	Ratio notes	**OH $R_{S/O}$**	**HO_2 $R_{S/O}$**	Other references targeting the same site
Underprediction	Hofzumahaus et al., 2009; Lu et al., 2012;	July 2006	BackGarden	Rural	Peaks (Mean)	15	15	Mean (Range, NO < 1 ppb) Mean (Lu et al., 2012)	0.2 to 0.33 0.5	N/A	N/A
Underprediction	Whalley et al., 2011	Apr–May 2008	DanumValley	Rainforest	Peaks (Mean)	2.5	3	w/C_5H_8 recycling mechanism (Peeters et al,. 2009)	~0.63	~0.5	Pugh et al., 2010
Underprediction	Liao et al., 2011	May–June 2007 Jun–Jul 2008	Summit	Polar	Mean (2007 spring) Mean (2008 summer)	3.0 4.1	2.7* 4.2*	2007 spring w/o BrO & w BrO 2008 summer w/o BrO & w BrO	0.72 0.78 0.54 0.56	0.87 0.96	Sjostedt et al., 2007
Underprediction	Wolfe et al., 2014	Aug 2010	Manitou	Forest	Peaks (Range)	3 to 10	24.6 to 44.3	Peak	~0.625	0.33	Kim et al., 2013
Underprediction	Tan et al., 2019	Oct–Nov 2014	Heshan	Suburban	Peaks (Mean)	4.5	3	Budget analysis only	N/A	1	N/A
Underprediction	Griffith et al., 2013	Jul–Aug 2008 Jul–Aug 2009	UMBS	Forest	Peak (Mean, 2008) Peak (Mean, 2009)	~3.3 ~1.6	~7 ~4.8	Mean (2008) Mean (2008 w/ISOP mechanisms) Mean (2009) Mean (2009 w/ISOP mechanisms)	~0.4 0.9	~0.57 ~1.3 ~0.6 ~1.5	N/A
Underprediction	Lu et al., 2013	Sept 2006	Yufa	Urban	Peaks (Range) Peaks (Mean)	4 to 17 ~7	2 to 24 ~1.5	Mean (NO < 0.1 ppb) Mean (NO > 1 ppb)	0.38 ~1	~1 ~1	N/A
Underprediction	Mao et al., 2012	Jun–Jul 2009	BFRS	Forest	Peaks (Mean w/ interference) Peaks (Mean w/o interference)	~4.5 ~1.8	N/A	Mean (w/ interference) Mean (w/o interference)	0.32 0.71	N/A	N/A
Underprediction	Tan et al., 2017; Lu et al., 2019	Summer 2014	Wangdu	Rural	Peaks (Range noontime)	5 to 15	3 to 14	Mean (NO > 0.3 ppb) Mean (NO < 0.3 ppb, afternoon)	~1 0.5	10 (NO > 4 ppb) N/A	N/A
Underprediction	Lew et al., 2020	Jul 2015	IURTP	Forest	Peaks (Mean)	4	10	Mean (Daytime) Mean (Evening and morning)	0.83 0.50	1.10 to 1.32	N/A
Underprediction	Lelieveld et al., 2008	Oct 2005	AmazonSuriname	Forest (Flight)	Mean (Forest boundary) Mean (Forest free troposphere) Mean (Atlantic boundary) Mean (Atlantic free troposphere)	5.6 8.2 9.0 10.1	10.5 4.9 6.7 5.5	Mean (w/MIM: Mainz ISOP mechanism) Mean (w/MIM2+: extra 40% to 80% OH recycle)	0.1 to 0.2 ~1	N/A	N/A

Table S1. Continued

Comparison results (OH only)	Reference	Time	Location in Figure 1	Site types	Measurement notes	OH conc. 10^6 cm^{-3}	HO_2 conc. 10^8 cm^{-3}	Ratio notes	**OH $R_{S/O}$**	**HO_2 $R_{S/O}$**	Other references targeting the same site
Well Matched	Ren, 2003b, a	Jun–Aug 2001	NewYork	Urban	Peaks (Range) Peaks (Mean)	2 to 20 7	0.5 to 6 1	Mean	0.91	0.81	N/A
Well Matched	Ren et al., 2006	Jul–Aug 2002	Whiteface	Forest	Peaks (Mean)	2.6	4.9	Mean	1.22	0.83	N/A
Well Matched	Kanaya et al., 2007b	Jan–Feb & Jul–Aug 2004	Tokyo	Urban	Peaks (Mean, winter) Peaks (Mean, summer)	1.5 6.3	0.27 1.4	Peaks (Mean, winter) Peaks (Mean, summer)	0.99 0.81	0.71 1.22	N/A
Well Matched	Feiner et al., 2016; Kaiser et al., 2016;	Jun–Jul 2013	Alabama	Forest	Peaks (Mean)	1	6.64	Peaks (Mean)	~1	~1	N/A
Well Matched	Jeong et al., 2022	Feb–Mar 2014	AmazonBrazil	Forest	Peaks (Mean 10:00-15:00) Peaks (Range)	1 ~1 to ~2.8	N/A	Mean	1	N/A	N/A
Well Matched	Hens et al., 2014	Summer 2010	Hyytiälä	Forest	Mean (Above-Canopy) Mean (Ground)	3.5 ~1.8 to ~1.2	N/A	Mean	1	0.3	Petäjä et al., 2009; Novelli et al., 2014;
Well Matched	Emmerson et al., 2007	Jul–Aug 2003	WrittleCollege	Urban	Peaks (Range)	1.2 to 7.5	0.16 to 3.3	Mean	1.24	1.07	N/A
Well Matched	Ren et al., 2013	Apr–May 2009	Houston	Urban	Peak (Mean)	~8.8	~6.2	Mean	0.9	1.22	Mao et al., 2010; Chen et al., 2010;
Well Matched	Ma et al., 2019	Nov–Dec 2017	PKU	Urban	Peaks (Mean clean) Peaks (Mean polluted)	2 1.5	0.4 0.3	Mean (clean) Mean (polluted)	~1 ~0.66	~0.66 0.08	N/A
Well Matched with missing source	Whalley et al., 2021	Summer 2017	IAP	Urban	Peak (All)	28	10	Mean (NO < 1 ppb)	~1	1.83	Slater et al., 2020
Well Matched with underpredicted HO_2	Zhang et al., 2022b	Nov–Dec 2019	Shanghai	Urban	Peaks (Mean)	2.7	0.8	N/A	N/A	N/A	N/A
No comparison	Kukui et al., 2008	June–July 2007	Grignon	Suburban	Peak (July 6)	~23	~2	N/A	N/A	N/A	N/A
No comparison	Wang et al., 2021	Oct–Nov 2018	PKUSZ	Suburban	Peaks (Mean)	5.3	4.2	N/A	N/A	N/A	Wang et al., 2019
No comparison	Rohrer and Berresheim, 2006	1999–2003	MOHp	Rural	Mean (All)	1.97	N/A	N/A	N/A	N/A	Handisides, 2003; Novelli et al., 2014;
No comparison	Zhang et al., 2022a	Aug–Sept 2019	Chengdu	Urban	Peaks (Range, PKU-LIF) Peaks (Range, AIOFM-LIF)	1.6 to 15 2.1 to 15.9	N/A	N/A	N/A	N/A	N/A

Notes:

ISOP:	Isoprene.
AIOFM:	Laser-induced fluorescence instrument by the Anhui Institute of Optics Fine Mechanics, Chinese Academy of Sciences.
Mean:	Campaign average concentration or ratio.
Peak:	Campaign maximum concentration or ratio.
Peaks (Mean):	Maximum concentration or ratio for the averaged diurnal or averaged cases.
Mean (Range):	Daily average concentration or ratio range for the campaign or cases.
Peaks (Range):	Maximum concentration or ratio range for the campaign or cases
w/ and w/o:	Considered or did not consider the specific mechanism, species, or interference.
~:	The result is based on the figure or description, and the exact number is not mentioned in the article.
N/A:	Not available in the article
*:	The HO_2 result includes some RO_2 species.

Calibration

The calibration was performed by applying the calibrator shown in Figure 2 to the CIMS. The calibration flow passes through the water bubbler and carries H_2O. When the humid calibration flow is exposed to the Pen Ray mercury lamp (Analytik Jena, UVP Pen Ray), the OH radicals produced by H_2O photolysis as shown below:

$$H_2O + hv(184.9\,nm) \rightarrow H + OH \quad \text{(SR1)}$$

The OH concentration ($[OH]$) produced by the calibrator is calculated by SE1.

$$[OH] = [H_2O] * \sigma_{H_2O} * \Phi * It \quad \text{(SE1)}$$

$[H_2O]$ is the water concentration in the calibration flow which is calculated from the temperature, saturated water vapor pressure, and relative humidity. σ_{H_2O} (= 7.14×10^{-20} cm^2; (Cantrell et al., 1997) is the photolysis cross-section of water vapor, while Φ represents the photolysis quantum yield and was assumed to be 1 (Kürten et al., 2012). The photon flux (It) was determined using the chemical actinometry method. This method measures the mixing ratio of N_2O and its photolysis products to determine the product It value of the lamp in the calibrator while the N_2O photolysis and H_2O photolysis require the same photon intensity (184.9 nm). The reactions and equations of It determination were presented by (Kürten et al., 2012). In this study, the It values were measured before and after the field campaign and no significant difference was found.

By calculating the $[OH]_{CAL}$ produced by the calibrator, the signal response to OH (TS_{97} - BS_{97}), and reagent ion (S_{62}), the calibration factor (C) can be calculated by following the equation which was transformed from E1.

$$C = \frac{1}{[OH]_{CAL}} \times \frac{TS_{97} - BS_{97}}{S_{62}} \quad \text{(SE2)}$$

Detection limit

The detection limit can be calculated as follows,

$$DL = \frac{1}{C} \times n * \sigma\left(\frac{BS_{97}}{S_{62}}\right) \quad \text{(SE3)}$$

Where DL is the detection limit in cm^{-3}, C is the calibration factor, and n is the ratio of signal to noise S/N. $\sigma\left(\frac{BS_{97}}{S_{62}}\right)$ represents the standard deviation of the background measurement when

the scavenger was added through front injectors. The detection limit (S/N = 3, average time = 6 minutes) in the laboratory was approximately 1.7×10^5 molecule cm^{-3} on average.

Uncertainty calculation

The uncertainty of the instrument is calculated by the rules for propagation for the uncertainty.

Propagation Rules for Addition ($y = x_1 + x_2$): $$e_y = \sqrt{e_{x1}^2 + e_{x2}^2} \quad \text{(SE4)}$$

Propagation Rules for Multiplication ($y = x_1 \times x_2$): $$\frac{e_y}{y} = \sqrt{\left(\frac{e_{x1}}{x_1}\right)^2 + \left(\frac{e_{x2}}{x_2}\right)^2} \quad \text{(SE5)}$$

Where e_y, e_{x1}, e_{x2}, are the absolute uncertainty for y, x_1, and x_2.

Calibration Uncertainties

The calibration uncertainty is calculated by the uncertainties of all the parameters involved in the SE2 which includes the uncertainty of calculated OH radicals concentration and the precision of the measurements of signal at 62 m/z and 97 m/z. Due to the equation SE1, the uncertainty of OH radical ($[OH]_{CAL}$) will further be contributed by the uncertainty of *It* ~36%, σ_{H_2O} (~5%), ϕ_{H_2O} (<1%, Cantrell et al. 1997), and calculated water concentration based on the measured Temperature and relative humidity (~10%). The precision of the measurements signal at 62 m/z and 97 m/z ($\frac{TS_{97}-BS_{97}}{S_{62}}$) of the CIMS instrument (2σ) was 11% (for 6 min integration time). Considering all the above uncertainties and calculated by the rules (SE3 and SE4), the overall uncertainty for the calibration factor can be calculated by the well-known uncertainty formula. The uncertainty for the calibration factor was about 38% in this study.

Sensitivity optimization

The calibration factor (C) of the CIMS instrument to the OH radicals depends on the conversion efficiency of OH to H_2SO_4 in the chemical conversion region (E_{Conv}), the ionization efficiency of H_2SO_4 to HSO_4^- in chemical ionization region (E_{Ion}), and the ion-transmitted efficiency of HSO_4^- from sample inlet to mass spectrometer system (E_{Trans}):

$$C \sim E_{Conv} \cdot E_{Ion} \cdot E_{Trans}$$

E_{Conv} is dependent on the reaction time and the SO_2 concentration of the conversion reactions

(R1-3). However, the conversion time has to be relatively short (<1s) to avoid the interference of HO_2 recycling as mentioned by Berresheim et al. (2000). E_{Ion} is affected by the flow dynamics, which determines the mixing of flows, and the electric field inside the ionization region, which forces the $NO_3^- \cdot (HNO_3)_m \cdot (HO_2)_n$ primary ions to the center of the region for H_2SO_4 ionization. E_{Trans} is related to the N_2 buffer and induces an electric field in the pinhole area. On the other hand, E_{Trans} is proportional to the transmission of the neutral molecule and particles from sampling air to the mass spectrometer system which deteriorates the measurement and damages the mass spectrometer. Thus, the optimization should take both transmission efficiency and protection function into consideration.

In this study, the CIMS was optimized before the field campaign. The detailed specification was shown in Table S1. To maximize the E_{Conv}, 5 sccm SO_2 was added from the front injectors to the sample flow and the [SO_2] was around 12 ppm in the sample flow. The sample flow was 3727 sccm and the sample flow rate was 55 cm/s which means the reaction time for OH conversion is around 47 ms.

The reaction time affects the positive bias of OH arising from HO_2 + NO in the inlet. To estimate this bias, Tanner et al., (1997) calculated the OH produced by the HO_2 recycling reaction under different NO conditions (from < 60 ppt to 1-2 ppb) in the inlet by a box model. Their results showed that the positive bias of less than 0.5×10^6 cm^{-3} with a 60 ms conversion time, and the bias does not increase with the increase of NO concentration. Thus, the conversion time of 47 ms in our study should further reduce such positive bias.

We tested both C_3F_6 and C_3H_8 as scavenger gas for OH. We found that the C_3H_8 provided by our suppliers were questionable because the scavenging efficiency ($SE = \frac{TS97-BS97}{TS97} \times 100\%$) by C_3H_8 in the different cylinders and different suppliers varied from 30% to 98% although the cylinders were labelled with the same concentration. In contrast, C_3F_6 from different cylinders labelled with the same concentration gave consistent SE. Therefore, we chose C_3F_6 as the OH scavenger gas.

These parameters taking the E_{Conv} and the HO_2 interference mentioned above into consideration. Similarly, the sample/sheath flow ratio was adjusted to 0.3 and the voltages different between sample and sheath flow were adjusted to 48 V to achieve the maximum E_{Ion}.

Finally, the buffer flow was 440 sccm and the Pinhole voltage difference was 30 V for a better E_{Trans} and to prevent neutral molecules enter the mass spectrometer system at the same time.

Table S2. Technical details and specifications of the OH-CIMS

Efficiency Related	Parameters	Gas	Values	Units	Specification for Measurement	Values	Units
E_{Conv}	**Front Injection**	SO_2 (0.9%)	5	sccm	Sample Flow [SO_2]	12	ppm
	Pulse Valve	N_2	2	sccm	Cycle Duration (OH)	6	mins
		C_3F_6 (99.9%)	2	sccm	Scavenging Efficiency (OH)	92%	
	Rear Injection	C_3F_6 (99.9%)	2	sccm	Sample Flow [C_3F_6]	1072	ppm
		HNO_3	10	sccm	Reaction Time	47	ms
	Sample Flow		3.7	slpm	Sample Flow Speed	55	cm/s
E_{Ion}	**Sheath Flow**	Zero Air	12.6	slpm	Reynolds Number in Ionization Chamber	>4000 Turbulent flows	
		HNO_3	10	sccm			
		C_3F_6 (99.9%)	2	sccm	Sheath Flow [C_3F_6]	159	ppm
	Total Flow		16.8	slpm	Sheath Flow Speed	25	cm/s
	Sheath Voltages		-80	V	Voltages Difference for ionization	48	V
	Sample Voltages		-32	V			
E_{Trans}	**Buffer Gas**	N_2	440	sccm	Voltages Difference for transmission	80	V
	Buffer Voltages		-70	V			
	Pinhole Voltages		-40	V			
Cal	**Calibration Flow**		10	slpm	Calibration Factor (Reagent ion: NO_3^-)	$1.21*10^{-8}$	cm^3
	Flow Speed		65	cm/s			
	Product It Value		$8.8*10^{10}$	photon/cm^2			

Uncertainties			Detection Limit ($10^5 \times cm^{-3}$)		
	Sigma (σ)	2		In the lab (3σ)	1.7
	Calibration	38%		Daytime (3σ)	12
	Overall	44%		Nighttime (3σ)	8.5

Notes:

sccm – Standard cubic centimeters per minute. Slpm – Standard liter per minute.

Ppm – Parts per million V – Voltage

The zero air was produced by Model 111 Zero Air Supply (Thermo Fisher Scientific) with an air compressor.

Suppliers for N_2, SO_2, and C_3F_6: Scientific Gas Engineering Co. Ltd., HK.

OH reactivity calculation

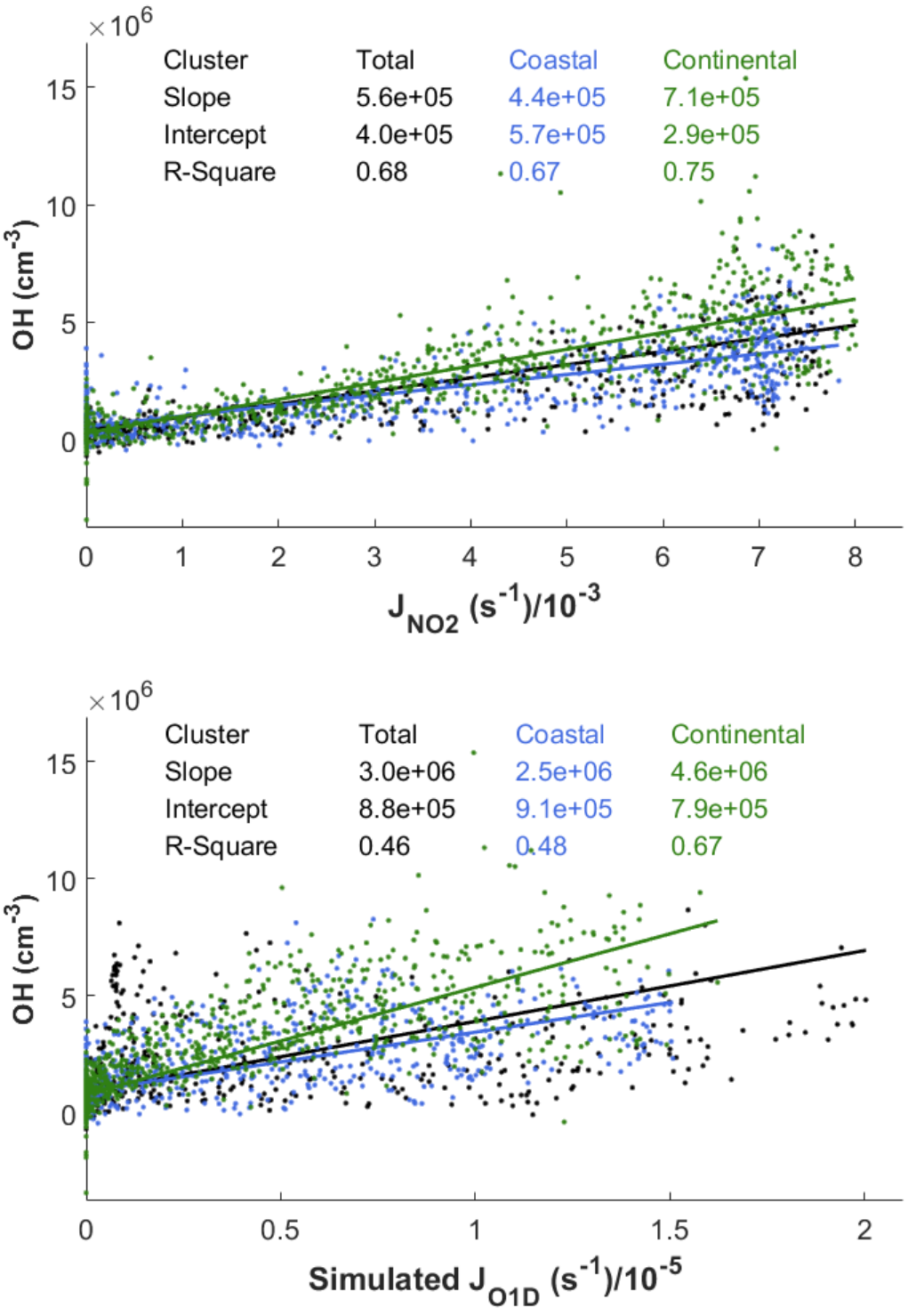

Figure S2. Correlation between observed OH concentration and a) photolysis frequency of NO_2 (J_{NO2}), and b) model simulated photolysis frequency O_3 (Simulated J_{O1D}). The linear regressions with respect to total, coastal, and continental cases are labelled in black, blue, and

green. Note that the coastal and continental cases are reported as correlations for all cases in different clusters, not only the selected cases in the Figures 6 and 8 comparisons.

Table S3. Average concentration with the standard deviations of measured species with respect to different cases.

Species Abb.	Species Name	Total	Coastal	Continental	Oct10M	Oct10A	Episode
OH 10^6 (cm^{-3})	Hydroxyl radical	2.4±1.9	2.5±1.4	3.1±1.7	3.7±2.1	1.8±1.5	4.2±2.8
OH_DL 10^6 (cm^{-3})	The detection limit of hydroxyl radical	1.0±0.5	0.8±0.3	0.9±0.3	1.2±0.5	1.5±0.7	1.0±0.5
OH_Err 10^6 (cm^{-3})	OH Measurement Uncertainty	1.5±1.0	1.8±0.5	1.7±0.6	0.9±0.8	1.0±0.9	2.5±1.7
PM_Num 10^3 (#/cm^3)	Number of particulate matters	3.8±1.9	4.1±1.7	4.9±1.4	NaN	NaN	5.6±2.0
*PM_Sur 10^7 (nm^2/cm^3)	The surface of particulate matters	19.7±9.0	15.0±2.3	26.8±4.3	NaN	NaN	31.5±14.2
PM_Vol 10^9 (nm^3/cm^3)	Volume of particulate matters	7.6±3.8	4.9±0.7	10.5±1.5	NaN	NaN	12.0±5.9
*RH (%)	Relative humidity	70.1±10.1	69.9±4.5	64.2±2.8	69.3±4.6	63.7±3.7	61.6±9.6
*CO2 (ppm)	Carbon dioxide	426.7±14.8	412.8±1.2	426.3±2.4	424.1±2.8	425.2±2.5	428.0±10.8
WindDi (°)	Wind direction	45.9±35.7	49.3±0.9	53.3±24.0	30.7±5.5	48.5±3.3	125.7±90.1
WindSp (m/s)	Wind speed	4.3±1.6	5.2±0.9	3.9±0.6	4.0±0.5	3.0±0.5	2.4±1.5
*Temp (°C)	Temperature	23.3±3.5	24.7±0.9	25.5±1.4	25.3±1.6	27.4±0.9	26.7±2.1
†SO2	Sulfur dioxide	2.6±1.2	3.2±0.2	3.4±0.1	3.5±0.2	3.2±0.1	4.4±0.8
†CO	Carbon monoxide	304.9±72	217.4±10.9	318.0±8.5	291.3±16.3	258.4±14.1	329.0±74.6
NH3	Ammonia	8.8±1.8	8.9±0.4	9.5±0.6	9.7±0.2	9.2±0.6	10.6±3.0
†NO	Nitrogen Monoxide	0.9±1.4	0.3±0.1	0.7±0.4	0.6±0.3	0.3±0.1	1.4±1.3
†NO2	Nitrogen Dioxide	3.9±3.5	1.6±0.7	4.5±1.1	3.4±1.4	1.1±0.5	10.1±5.6
†NOx	Nitrogen Oxides	4.8±4.4	1.9±0.7	5.2±1.2	4.0±1.6	1.4±0.5	11.4±6.2
†O3	Ozone	49.9±20.6	59.5±10.1	54.7±14.5	44.2±9.9	61.2±3.8	70.4±33.5
†JNO2 10^{-3} (s^{-1})	The photolysis rate constant of NO2	3.6±2.5	4.7±2.4	4.0±2.0	4.8±2.5	5.0±2.6	4.3±2.2

†HONO	Nitrous acid	0.15±0.069	0.15±0.019	0.16±0.035	0.29±0.101	0.14±0.015	NaN
*C2H4	Ethene	1.4±1.3	0.5±0.1	0.7±0.1	0.6±0.1	0.3±0.1	0.9±0.2
*C2H6	Ethane	1.9±0.9	1.4±0.1	2.1±0.1	2.0±0.1	1.7±0.1	2.3±0.5
*C3H8	Propane	1.7±0.9	1.1±0.2	1.5±0.2	1.3±0.1	0.8±0.1	2.1±1.7
*C3H6	Propene	0.10±0.05	0.07±0.01	0.11±0.02	0.18±0.06	0.06±0.01	0.12±0.04
*C2H2	Ethyne	1.63±0.65	0.97±0.03	1.42±0.23	1.07±0.08	NaN	1.39±0.48
*IC4H10	i-Butane	0.55±0.44	0.22±0.04	0.61±0.14	0.44±0.09	0.23±0.07	1.02±1.04
*NC4H10	n-Butane	0.76±0.60	0.27±0.06	0.88±0.19	0.67±0.13	0.32±0.08	1.53±1.62
*TBUT2ENE	But-2-ene	0.06±0.01	0.05±0.00	0.06±0.00	0.05±0.00	NaN	0.06±0.01
*BUT1ENE	But-1-ene	0.08±0.03	NaN	0.10±0.01	0.08±0.01	NaN	NaN
*IC5H12	i-Pentane	0.40±0.22	0.18±0.04	0.42±0.05	0.46±0.03	0.28±0.11	0.60±0.36
*NC5H12	n-Pentane	0.24±0.12	0.13±0.02	0.24±0.02	0.33±0.05	0.17±0.04	0.29±0.21
*C4H6	Buta-1,3-diene	0.06±0.01	NaN	0.06±0.00	NaN	NaN	0.06±0.00
*M2PE	2-Methyl pentane	0.31±0.14	NaN	0.28±0.05	0.30±0.04	0.20±0.00	0.36±0.27
*NC6H14	n-Hexane	0.15±0.11	0.08±0.01	0.15±0.04	0.10±0.03	0.05±0.00	0.28±0.28
*IC8H18	i-Octane	0.02±0.02	NaN	0.02±0.01	NaN	NaN	0.05±0.06
*NC7H16	n-Heptane	0.03±0.01	NaN	0.07±0.00	NaN	NaN	0.07±0.00
*NC8H18	n-Octane	0.03±0.00	NaN	0.03±0.00	NaN	NaN	0.03±0.00
*EBENZ	Ethyl Benzene	0.05±0.04	0.02±0.01	0.05±0.01	0.05±0.02	0.01±0.00	0.08±0.09
*MXYL	m-Xylene	0.03±0.03	0.01±0.00	0.03±0.01	0.03±0.01	0.01±0.00	0.02±0.02
*OXYL	o-Xylene	0.04±0.03	0.01±0.00	0.03±0.01	0.03±0.01	0.01±0.00	0.03±0.03
**CH2O2	Formic acid	1.02±0.44	0.58±0.08	1.03±0.19	1.16±0.20	1.55±0.11	1.54±0.47
**C2H4O2	Acetic acid	2.76±1.46	1.59±0.34	3.03±0.68	4.54±0.35	3.19±0.61	4.38±3.25
**C2H8O2	Ethylene dihydrate	0.06±0.02	0.06±0.00	0.06±0.01	0.05±0.00	0.04±0.00	0.09±0.06
**C5H8	Isoprene	0.31±0.24	0.16±0.06	0.36±0.14	0.69±0.46	0.56±0.33	0.54±0.25
**C4H6O	Methyl Vinyl Ketone+ Methacrolein	0.16±0.10	0.06±0.01	0.22±0.06	0.26±0.05	0.15±0.06	0.32±0.19
**C3H4O2	Acrylic acid	0.12±0.05	0.06±0.01	0.13±0.03	0.16±0.02	0.13±0.02	0.19±0.10
**C3H6O2	Propanoic acid/ Hydroxy acetone	0.90±0.43	0.57±0.15	0.97±0.23	1.26±0.03	1.01±0.11	1.45±0.93
**C6H6	Benzene	0.28±0.13	0.12±0.03	0.33±0.03	0.43±0.04	0.25±0.05	0.38±0.21
**C6H12	Cyclohexane	0.02±0.01	0.01±0.00	0.03±0.00	0.03±0.01	0.02±0.01	0.04±0.03
**C3H4O3	Pyruvic acid	0.05±0.02	0.03±0.00	0.05±0.01	0.07±0.01	0.07±0.00	0.06±0.03
**C7H8	Toluene	0.38±0.27	0.20±0.10	0.46±0.11	0.50±0.08	0.24±0.04	0.69±0.67
**C8H10	Xylene	0.25±0.22	0.09±0.08	0.35±0.07	0.49±0.17	0.07±0.05	0.41±0.34
**C10H16	Monoterpene	0.05±0.03	0.03±0.00	0.06±0.01	0.10±0.06	0.09±0.04	0.07±0.03
**CH2O	Formaldehyde	1.03±0.41	0.62±0.05	1.17±0.11	1.72±0.10	1.59±0.17	1.17±0.42
**C2H4O	Acetaldehyde	1.88±0.90	0.98±0.13	2.10±0.41	2.74±0.16	1.96±0.36	3.17±1.98
**C3H6O	Acetone	3.88±1.60	2.18±0.31	4.43±0.74	5.64±0.49	5.91±0.47	5.92±2.85
**C3H4O	Acrolein	0.25±0.11	0.14±0.02	0.29±0.05	0.39±0.04	0.33±0.05	0.39±0.19

**C4H8O	MEK + Butanals	0.45±0.30	0.24±0.04	0.53±0.16	0.59±0.05	0.44±0.05	0.87±0.86
**C8H8O	Methyl benzaldehyde	0.04±0.03	0.02±0.00	0.05±0.01	0.06±0.00	0.04±0.01	0.08±0.06
[&]BVOC	Biogenic VOCs	0.3±0.4	0.2±0.1	0.4±0.1	1.1±0.6	0.8±0.4	0.7±0.5
[&]AVOC	Anthropogenic VOCs	7.1±3.6	4.0±0.7	7.6±0.9	7.7±0.9	4.4±0.7	11.1±8.7
[&]OVOC	Oxygenated VOCs	7.2±7.4	7.0±1.0	9.2±1.5	18.6±1.3	16.4±1.9	14.9±12.8
[&]Arom	Aromatic compounds	0.6±0.6	0.4±0.2	0.8±0.1	1.5±0.3	0.6±0.1	1.2±1.3
[&]Alkane	Alkane	6.5±3.4	3.6±0.5	6.8±0.8	6.3±0.6	3.8±0.6	9.9±7.5
[&]Alkene	Alkene	2.5±1.9	0.5±0.1	2.2±0.2	2.6±0.2	1.0±0.5	2.5±1.0
[&]Aldehyde	Aldehyde	4.4±4.5	4.2±0.5	5.7±0.8	11.4±0.8	10.4±1.1	9.1±7.6
[&]Acid	Acid	2.8±2.9	2.8±0.5	3.4±0.6	7.2±0.5	5.9±0.8	5.8±5.2

Notes:

The concentration was averaged from the daytime (6:00 to 18:00) results.

The concentration unit is presented in the bracket in the 'Species Abb.'.

The unit for other species is in ppb.

* Species measured by GC-MS and constrained by the model

** Species measured by PTR-MS and constrained by the model.

[†] Species measured by instrument specified in Table 1.

[&] Different VOCs functional groups.

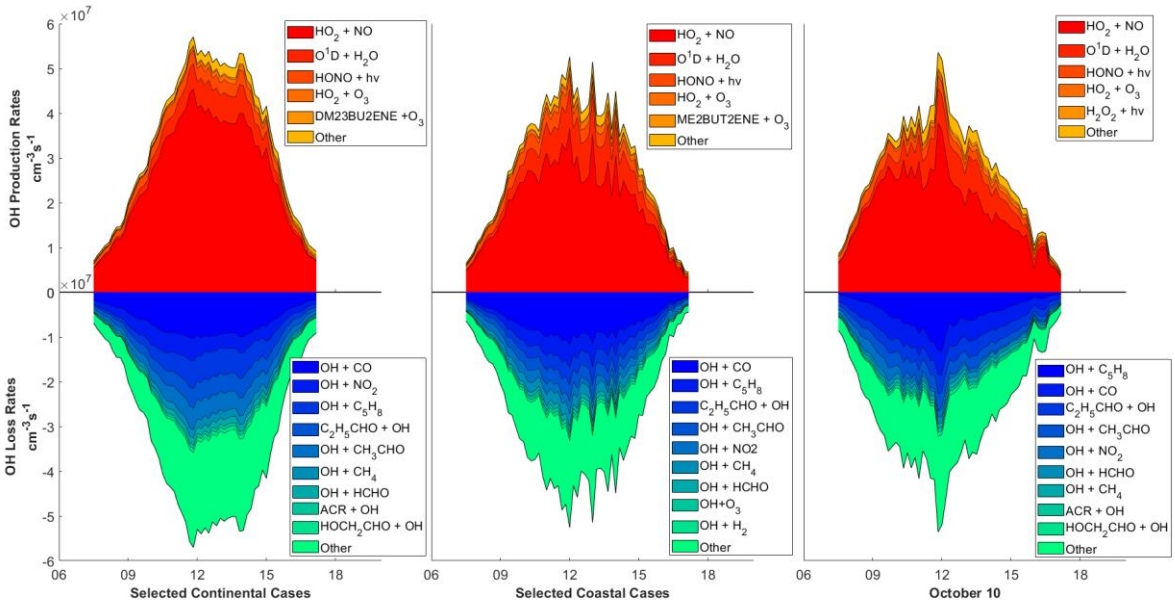

Figure S3. OH radical budgets for the continental cases, coastal cases, and 10 October. Where DM23BU2ENE and ME2BUT2ENE represent 2,3-Dimethyl-2-butene and 2-Methyl-2-butene respectively.

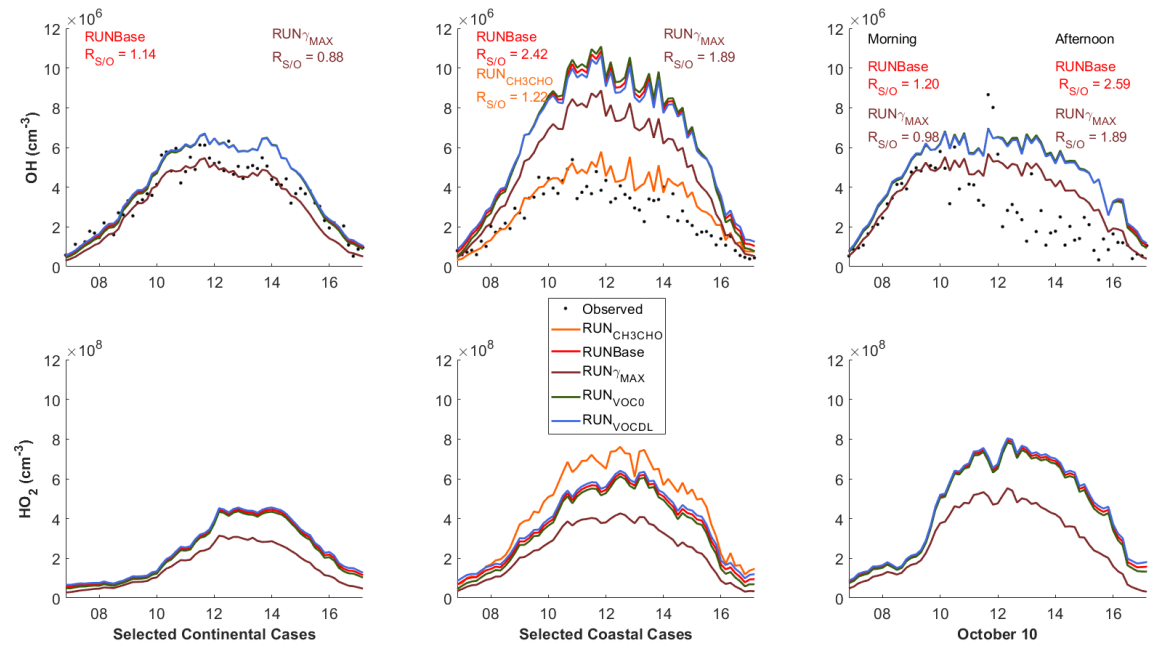

Figure S4. Sensitivity tests for the simulated OH and HO_2 in continental and coastal cases and on 10 October. RUN_{CH3CHO} shows the simulated results of the selected coastal cases when additional CH_3CHO is added as OH sinks. $RUN\gamma_{MAX}$ shows the simulated results for the

maximum heterogeneous uptake effect of HO_2 ($\gamma = 1$). The RUN_{VOC0} and RUN_{VOCDL} show the simulated results that constraints "0" and the detection limit value as the concentration of VOCs when their concentration was below detection limits.

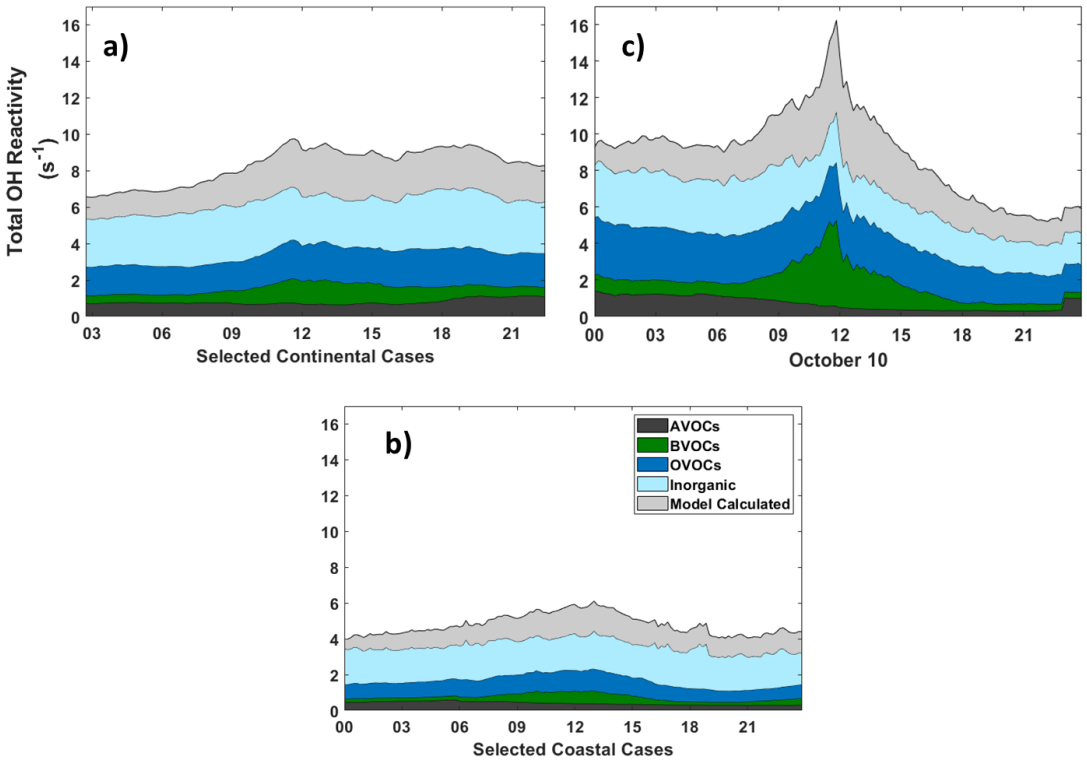

Figure S5. Simulated reactivity for continental cases (a), coastal cases (b), and 10 October (c). The AVOCs, BVOCs, OVOCs, and Inorganic demonstrate the reactivity calculated from the measured species and the Model Calculated represents the reactivity calculated by the derived species simulated by the model.

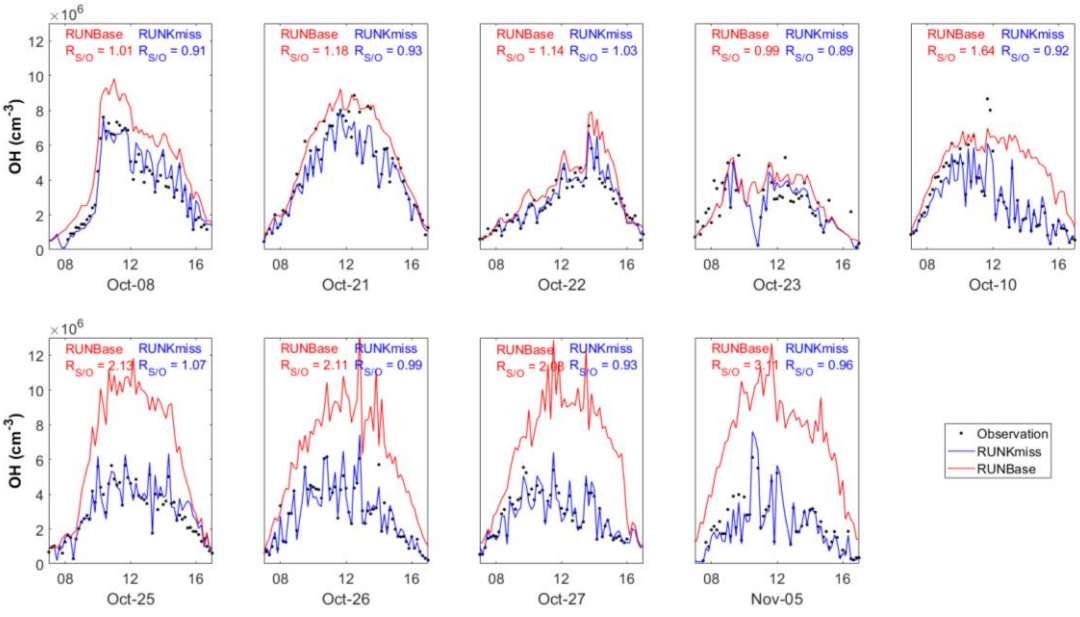

Figure S6. Nine-day comparison between observed OH and simulated OH with (RUNBase) and without (RUNKmiss) addition reactivity.

Reference:

Berresheim, H., Elste, T., Tremmel, H. G., Allen, A. G., Hansson, H.-C., Rosman, K., Dal Maso, M., Mäkelä, J. M., Kulmala, M., and O'Dowd, C. D.: Gas-aerosol relationships of H_2SO_4, MSA, and OH: Observations in the coastal marine boundary layer at Mace Head, Ireland, Journal of Geophysical Research: Atmospheres, 107, PAR 5-1-PAR 5-12, https://doi.org/10.1029/2000JD000229, 2002.

Berresheim, H., McGrath, J., Adam, M., Mauldin, R. L., Bohn, B., and Rohrer, F.: Seasonal measurements of OH, NO_x, and $J(O^1D)$ at Mace Head, Ireland, Geophys. Res. Lett., 40, 1659–1663, https://doi.org/10.1002/grl.50345, 2013.

Berresheim, H., Adam, M., Monahan, C., O'Dowd, C., Plane, J. M. C., Bohn, B., and Rohrer, F.: Missing SO_2 oxidant in the coastal atmosphere? – observations from high-resolution measurements of OH and atmospheric sulfur compounds, Atmospheric Chemistry and Physics, 14, 12209–12223, https://doi.org/10.5194/acp-14-12209-2014, 2014.

Bloss, W. J., Lee, J. D., Heard, D. E., Salmon, R. A., Bauguitte, S. J.-B., Roscoe, H. K., and Jones, A. E.: Observations of OH and HO_2 radicals in coastal Antarctica, Atmospheric Chemistry and Physics, 7, 4171–4185, https://doi.org/10.5194/acp-7-4171-2007, 2007.

Cantrell, C. A., Zimmer, A., and Tyndall, G. S.: Absorption cross sections for water vapor from 183 to 193 nm, Geophys. Res. Lett., 24, 2195–2198, https://doi.org/10.1029/97GL02100, 1997.

Carslaw, N., Creasey, D. J., Heard, D. E., Lewis, A. C., McQuaid, J. B., Pilling, M. J., Monks, P. S., Bandy, B. J., and Penkett, S. A.: Modeling OH, HO_2, and RO_2 radicals in the marine boundary layer: 1. Model construction and comparison with field measurements, J. Geophys. Res., 104, 30241–30255, https://doi.org/10.1029/1999JD900783, 1999.

Chen, S., Ren, X., Mao, J., Chen, Z., Brune, W. H., Lefer, B., Rappenglück, B., Flynn, J., Olson, J., and Crawford, J. H.: A comparison of chemical mechanisms based on TRAMP-2006 field data, Atmospheric Environment, 44, 4116–4125, https://doi.org/10.1016/j.atmosenv.2009.05.027, 2010.

Creasey, D. J., Evans, G. E., and Heard, D. E.: Measurements of OH and HO_2 concentrations in the Southern Ocean marine boundary layer, J. Geophys. Res., 108, 4475, https://doi.org/10.1029/2002JD003206, 2003.

Dusanter, S., Vimal, D., Stevens, P. S., Volkamer, R., and Molina, L. T.: Measurements of OH and HO_2 concentrations during the MCMA-2006 field campaign – Part 1: Deployment of the Indiana University laser-induced fluorescence instrument, Atmospheric Chemistry and Physics, 9, 1665–1685, https://doi.org/10.5194/acp-9-1665-2009, 2009a.

Dusanter, S., Vimal, D., Stevens, P. S., Volkamer, R., Molina, L. T., Baker, A., Meinardi, S., Blake, D.,

Sheehy, P., Merten, A., Zhang, R., Zheng, J., Fortner, E. C., Junkermann, W., Dubey, M., Rahn, T., Eichinger, B., Lewandowski, P., Prueger, J., and Holder, H.: Measurements of OH and HO_2 concentrations during the MCMA-2006 field campaign – Part 2: Model comparison and radical budget, Atmospheric Chemistry and Physics, 9, 6655–6675, https://doi.org/10.5194/acp-9-6655-2009, 2009b.

Emmerson, K. M., Carslaw, N., Carslaw, D. C., Lee, J. D., McFiggans, G., Bloss, W. J., Gravestock, T., Heard, D. E., Hopkins, J., Ingham, T., Pilling, M. J., Smith, S. C., Jacob, M., and Monks, P. S.: Free radical modelling studies during the UK TORCH Campaign in Summer 2003, Atmos. Chem. Phys., 15, 2007.

Feiner, P. A., Brune, W. H., Miller, D. O., Zhang, L., Cohen, R. C., Romer, P. S., Goldstein, A. H., Keutsch, F. N., Skog, K. M., Wennberg, P. O., Nguyen, T. B., Teng, A. P., DeGouw, J., Koss, A., Wild, R. J., Brown, S. S., Guenther, A., Edgerton, E., Baumann, K., and Fry, J. L.: Testing Atmospheric Oxidation in an Alabama Forest, Journal of the Atmospheric Sciences, 73, 4699–4710, https://doi.org/10.1175/JAS-D-16-0044.1, 2016.

Griffith, S. M., Hansen, R. F., Dusanter, S., Stevens, P. S., Alaghmand, M., Bertman, S. B., Carroll, M. A., Erickson, M., Galloway, M., Grossberg, N., Hottle, J., Hou, J., Jobson, B. T., Kammrath, A., Keutsch, F. N., Lefer, B. L., Mielke, L. H., O'Brien, A., Shepson, P. B., Thurlow, M., Wallace, W., Zhang, N., and Zhou, X. L.: OH and HO_2 radical chemistry during PROPHET 2008 and CABINEX 2009 - Part 1: Measurements and model comparison, Atmospheric Chemistry and Physics, 13, 5403–5423, https://doi.org/10.5194/acp-13-5403-2013, 2013.

Griffith, S. M., Hansen, R. F., Dusanter, S., Michoud, V., Gilman, J. B., Kuster, W. C., Veres, P. R., Graus, M., Gouw, J. A., Roberts, J., Young, C., Washenfelder, R., Brown, S. S., Thalman, R., Waxman, E., Volkamer, R., Tsai, C., Stutz, J., Flynn, J. H., Grossberg, N., Lefer, B., Alvarez, S. L., Rappenglueck, B., Mielke, L. H., Osthoff, H. D., and Stevens, P. S.: Measurements of hydroxyl and hydroperoxy radicals during CalNex-LA: Model comparisons and radical budgets, J. Geophys. Res. Atmos., 121, 4211–4232, https://doi.org/10.1002/2015JD024358, 2016.

Handisides, G. M.: Hohenpeissenberg Photochemical Experiment (HOPE 2000): Measurements and photostationary state calculations of OH and peroxy radicals, Atmos. Chem. Phys., 24, 2003.

Hens, K., Novelli, A., Martinez, M., Auld, J., Axinte, R., Bohn, B., Fischer, H., Keronen, P., Kubistin, D., Nölscher, A. C., Oswald, R., Paasonen, P., Petäjä, T., Regelin, E., Sander, R., Sinha, V., Sipilä, M., Taraborrelli, D., Tatum Ernest, C., Williams, J., Lelieveld, J., and Harder, H.: Observation and modelling of HO_x radicals in a boreal forest, Atmospheric Chemistry and Physics, 14, 8723–8747, https://doi.org/10.5194/acp-14-8723-2014, 2014.

Hofzumahaus, A., Rohrer, F., Lu, K., Bohn, B., Brauers, T., Chang, C.-C., Fuchs, H., Holland, F., Kita, K., Kondo, Y., Li, X., Lou, S., Shao, M., Zeng, L., Wahner, A., and Zhang, Y.: Amplified Trace Gas Removal in the Troposphere, Science, 324, 1702–1704, https://doi.org/10.1126/science.1164566, 2009.

Holland, F., Hofzumahaus, A., Schäfer, J., and Kraus, A.: Measurements of OH and HO_2 radical concentrations and photolysis frequencies during BERLIOZ, J. Geophys. Res., 108, 8246, https://doi.org/10.1029/2001JD001393, 2003.

Jeong, D., Seco, R., Emmons, L., Schwantes, R., Liu, Y., McKinney, K. A., Martin, S. T., Keutsch, F. N., Gu, D., Guenther, A. B., Vega, O., Tota, J., Souza, R. A. F., Springston, S. R., Watson, T. B., and Kim, S.: Reconciling Observed and Predicted Tropical Rainforest OH Concentrations, JGR Atmospheres, 127, https://doi.org/10.1029/2020JD032901, 2022.

Kaiser, J., Skog, K. M., Baumann, K., Bertman, S. B., Brown, S. B., Brune, W. H., Crounse, J. D., de Gouw, J. A., Edgerton, E. S., Feiner, P. A., Goldstein, A. H., Koss, A., Misztal, P. K., Nguyen, T. B., Olson, K. F., St. Clair, J. M., Teng, A. P., Toma, S., Wennberg, P. O., Wild, R. J., Zhang, L., and Keutsch, F. N.: Speciation of OH reactivity above the canopy of an isoprene-dominated forest, Atmos. Chem. Phys., 16, 9349–9359, https://doi.org/10.5194/acp-16-9349-2016, 2016.

Kanaya, Y., Cao, R., Kato, S., Miyakawa, Y., Kajii, Y., Tanimoto, H., Yokouchi, Y., Mochida, M., Kawamura, K., and Akimoto, H.: Chemistry of OH and HO_2 radicals observed at Rishiri Island, Japan, in September 2003: Missing daytime sink of HO_2 and positive nighttime correlations with monoterpenes, J. Geophys. Res., 112, D11308, https://doi.org/10.1029/2006JD007987, 2007a.

Kanaya, Y., Cao, R., Akimoto, H., Fukuda, M., Komazaki, Y., Yokouchi, Y., Koike, M., Tanimoto, H., Takegawa, N., and Kondo, Y.: Urban photochemistry in central Tokyo: 1. Observed and modeled OH and HO_2 radical concentrations during the winter and summer of 2004, J. Geophys. Res., 112, D21312, https://doi.org/10.1029/2007JD008670, 2007b.

Kim, S., Wolfe, G. M., Mauldin, L., Cantrell, C., Guenther, A., Karl, T., Turnipseed, A., Greenberg, J., Hall, S. R., Ullmann, K., Apel, E., Hornbrook, R., Kajii, Y., Nakashima, Y., Keutsch, F. N., DiGangi, J. P., Henry, S. B., Kaser, L., Schnitzhofer, R., Graus, M., Hansel, A., Zheng, W., and Flocke, F. F.: Evaluation of HO_x sources and cycling using measurement-constrained model calculations in a 2-methyl-3-butene-2-ol (MBO) and monoterpene (MT) dominated ecosystem, Atmospheric Chemistry and Physics, 13, 2031–2044, https://doi.org/10.5194/acp-13-2031-2013, 2013.

Kukui, A., Ancellet, G., and Le Bras, G.: Chemical ionisation mass spectrometer for measurements of OH and Peroxy radical concentrations in moderately polluted atmospheres, J Atmos Chem, 61, 133–154, https://doi.org/10.1007/s10874-009-9130-9, 2008.

Kukui, A., Legrand, M., Preunkert, S., Frey, M. M., Loisil, R., Gil Roca, J., Jourdain, B., King, M. D., France, J. L., and Ancellet, G.: Measurements of OH and RO_2 radicals at Dome C, East Antarctica, Atmospheric Chemistry and Physics, 14, 12373–12392, https://doi.org/10.5194/acp-14-12373-2014, 2014.

Kürten, A., Rondo, L., Ehrhart, S., and Curtius, J.: Calibration of a Chemical Ionization Mass Spectrometer for the Measurement of Gaseous Sulfuric Acid, J. Phys. Chem. A, 116, 6375–6386, https://doi.org/10.1021/jp212123n, 2012.

Lelieveld, J., Butler, T. M., Crowley, J. N., Dillon, T. J., Fischer, H., Ganzeveld, L., Harder, H., Lawrence, M. G., Martinez, M., Taraborrelli, D., and Williams, J.: Atmospheric oxidation capacity sustained by a tropical forest, Nature, 452, 737–740, https://doi.org/10.1038/nature06870, 2008.

Lew, M. M., Rickly, P. S., Bottorff, B. P., Reidy, E., Sklaveniti, S., Léonardis, T., Locoge, N., Dusanter, S., Kundu, S., Wood, E., and Stevens, P. S.: OH and HO_2 radical chemistry in a midlatitude forest:

measurements and model comparisons, Atmospheric Chemistry and Physics, 20, 9209–9230, https://doi.org/10.5194/acp-20-9209-2020, 2020.

Liao, J., Huey, L. G., Tanner, D. J., Brough, N., Brooks, S., Dibb, J. E., Stutz, J., Thomas, J. L., Lefer, B., Haman, C., and Gorham, K.: Observations of hydroxyl and peroxy radicals and the impact of BrO at Summit, Greenland in 2007 and 2008, Atmos. Chem. Phys., 11, 8577–8591, https://doi.org/10.5194/acp-11-8577-2011, 2011.

Lu, K., Fuchs, H., Hofzumahaus, A., Tan, Z., Wang, H., Zhang, L., Schmitt, S. H., Rohrer, F., Bohn, B., Broch, S., Dong, H., Gkatzelis, G. I., Hohaus, T., Holland, F., Li, X., Liu, Y., Liu, Y., Ma, X., Novelli, A., Schlag, P., Shao, M., Wu, Y., Wu, Z., Zeng, L., Hu, M., Kiendler-Scharr, A., Wahner, A., and Zhang, Y.: Fast Photochemistry in Wintertime Haze: Consequences for Pollution Mitigation Strategies, Environ. Sci. Technol., 53, 10676–10684, https://doi.org/10.1021/acs.est.9b02422, 2019.

Lu, K. D., Rohrer, F., Holland, F., Fuchs, H., Bohn, B., Brauers, T., Chang, C. C., Häseler, R., Hu, M., Kita, K., Kondo, Y., Li, X., Lou, S. R., Nehr, S., Shao, M., Zeng, L. M., Wahner, A., Zhang, Y. H., and Hofzumahaus, A.: Observation and modelling of OH and HO_2 concentrations in the Pearl River Delta 2006: a missing OH source in a VOC rich atmosphere, Atmospheric Chemistry and Physics, 12, 1541–1569, https://doi.org/10.5194/acp-12-1541-2012, 2012.

Lu, K. D., Hofzumahaus, A., Holland, F., Bohn, B., Brauers, T., Fuchs, H., Hu, M., Häseler, R., Kita, K., Kondo, Y., Li, X., Lou, S. R., Oebel, A., Shao, M., Zeng, L. M., Wahner, A., Zhu, T., Zhang, Y. H., and Rohrer, F.: Missing OH source in a suburban environment near Beijing: observed and modelled OH and HO_2 concentrations in summer 2006, Atmospheric Chemistry and Physics, 13, 1057–1080, https://doi.org/10.5194/acp-13-1057-2013, 2013.

Ma, X., Tan, Z., Lu, K., Yang, X., Liu, Y., Li, S., Li, X., Chen, S., Novelli, A., Cho, C., Zeng, L., Wahner, A., and Zhang, Y.: Winter photochemistry in Beijing: Observation and model simulation of OH and HO2 radicals at an urban site, Science of The Total Environment, 685, 85–95, https://doi.org/10.1016/j.scitotenv.2019.05.329, 2019.

Mao, J., Ren, X., Chen, S., Brune, W. H., Chen, Z., Martinez, M., Harder, H., Lefer, B., Rappenglück, B., Flynn, J., and Leuchner, M.: Atmospheric oxidation capacity in the summer of Houston 2006: Comparison with summer measurements in other metropolitan studies, Atmospheric Environment, 44, 4107–4115, https://doi.org/10.1016/j.atmosenv.2009.01.013, 2010.

Mao, J., Ren, X., Zhang, L., Van Duin, D. M., Cohen, R. C., Park, J.-H., Goldstein, A. H., Paulot, F., Beaver, M. R., Crounse, J. D., Wennberg, P. O., DiGangi, J. P., Henry, S. B., Keutsch, F. N., Park, C., Schade, G. W., Wolfe, G. M., Thornton, J. A., and Brune, W. H.: Insights into hydroxyl measurements and atmospheric oxidation in a California forest, Atmos. Chem. Phys., 12, 8009–8020, https://doi.org/10.5194/acp-12-8009-2012, 2012.

Mauldin III, R., Kosciuch, E., Eisele, F., Huey, G., Tanner, D., Sjostedt, S., Blake, D., Chen, G., Crawford, J., and Davis, D.: South Pole Antarctica observations and modeling results: New insights on HO_x radical and sulfur chemistry, Atmospheric Environment, 44, 572–581, https://doi.org/10.1016/j.atmosenv.2009.07.058, 2010.

Mauldin III, R. L., Eisele, F. L., Tanner, D. J., Kosciuch, E., Shetter, R., Lefer, B., Hall, S. R., Nowak, J. B., Buhr, M., Chen, G., Wang, P., and Davis, D.: Measurements of OH, H_2SO_4, and MSA at the South Pole during ISCAT, Geophysical Research Letters, 28, 3629–3632, https://doi.org/10.1029/2000GL012711, 2001.

Novelli, A., Vereecken, L., Lelieveld, J., and Harder, H.: Direct observation of OH formation from stabilised Criegee intermediates, Phys. Chem. Chem. Phys., 16, 19941–19951, https://doi.org/10.1039/C4CP02719A, 2014.

Petäjä, T., Mauldin, I. I. I., Kosciuch, E., McGrath, J., Nieminen, T., Paasonen, P., Boy, M., Adamov, A., Kotiaho, T., and Kulmala, M.: Sulfuric acid and OH concentrations in a boreal forest site, Atmospheric Chemistry and Physics, 9, 7435–7448, https://doi.org/10.5194/acp-9-7435-2009, 2009.

Pugh, T. A. M., MacKenzie, A. R., Hewitt, C. N., Langford, B., Edwards, P. M., Furneaux, K. L., Heard, D. E., Hopkins, J. R., Jones, C. E., Karunaharan, A., Lee, J., Mills, G., Misztal, P., Moller, S., Monks, P. S., and Whalley, L. K.: Simulating atmospheric composition over a South-East Asian tropical rainforest: performance of a chemistry box model, Atmos. Chem. Phys., 20, 2010.

Ren, X.: HO_x concentrations and OH reactivity observations in New York City during PMTACS-NY2001, Atmospheric Environment, 37, 3627–3637, https://doi.org/10.1016/S1352-2310(03)00460-6, 2003a.

Ren, X.: OH and HO_2 Chemistry in the urban atmosphere of New York City, Atmospheric Environment, 37, 3639–3651, https://doi.org/10.1016/S1352-2310(03)00459-X, 2003b.

Ren, X., Brune, W. H., Oliger, A., Metcalf, A. R., Simpas, J. B., Shirley, T., Schwab, J. J., Bai, C., Roychowdhury, U., Li, Y., Cai, C., Demerjian, K. L., He, Y., Zhou, X., Gao, H., and Hou, J.: OH, HO_2 , and OH reactivity during the PMTACS-NY Whiteface Mountain 2002 campaign: Observations and model comparison: HO_x DURING PMTACS-NY WHITEFACE 2002, J. Geophys. Res., 111, n/a-n/a, https://doi.org/10.1029/2005JD006126, 2006.

Ren, X., van Duin, D., Cazorla, M., Chen, S., Mao, J., Zhang, L., Brune, W. H., Flynn, J. H., Grossberg, N., Lefer, B. L., Rappenglück, B., Wong, K. W., Tsai, C., Stutz, J., Dibb, J. E., Thomas Jobson, B., Luke, W. T., and Kelley, P.: Atmospheric oxidation chemistry and ozone production: Results from SHARP 2009 in Houston, Texas: ATMOSPHERIC PHOTOCHEMISTRY IN HOUSTON, J. Geophys. Res. Atmos., 118, 5770–5780, https://doi.org/10.1002/jgrd.50342, 2013.

Rohrer, F. and Berresheim, H.: Strong correlation between levels of tropospheric hydroxyl radicals and solar ultraviolet radiation, Nature, 442, 184–187, https://doi.org/10.1038/nature04924, 2006.

Sjostedt, S. J., Huey, L. G., Tanner, D. J., Peischl, J., Chen, G., Dibb, J. E., Lefer, B., Hutterli, M. A., Beyersdorf, A. J., Blake, N. J., Blake, D. R., Sueper, D., Ryerson, T., Burkhart, J., and Stohl, A.: Observations of hydroxyl and the sum of peroxy radicals at Summit, Greenland during summer 2003, Atmospheric Environment, 41, 5122–5137, https://doi.org/10.1016/j.atmosenv.2006.06.065, 2007.

Slater, E. J., Whalley, L. K., Woodward-Massey, R., Ye, C., Lee, J. D., Squires, F., Hopkins, J. R., Dunmore, R. E., Shaw, M., Hamilton, J. F., Lewis, A. C., Crilley, L. R., Kramer, L., Bloss, W., Vu, T., Sun, Y., Xu, W.,

Yue, S., Ren, L., Acton, W. J. F., Hewitt, C. N., Wang, X., Fu, P., and Heard, D. E.: Elevated levels of OH observed in haze events during wintertime in central Beijing, Atmospheric Chemistry and Physics, 20, 14847–14871, https://doi.org/10.5194/acp-20-14847-2020, 2020.

Sommariva, R., Lewis, A. C., Pilling, M. J., and Zador, J.: OH and HO_2 chemistry in clean marine air during SOAPEX-2, Atmos. Chem. Phys., 18, 2004.

Tan, Z., Fuchs, H., Lu, K., Hofzumahaus, A., Bohn, B., Broch, S., Dong, H., Gomm, S., Häseler, R., He, L., Holland, F., Li, X., Liu, Y., Lu, S., Rohrer, F., Shao, M., Wang, B., Wang, M., Wu, Y., Zeng, L., Zhang, Y., Wahner, A., and Zhang, Y.: Radical chemistry at a rural site (Wangdu) in the North China Plain: observation and model calculations of OH, HO_2 and RO_2 radicals, Atmospheric Chemistry and Physics, 17, 663–690, https://doi.org/10.5194/acp-17-663-2017, 2017.

Tan, Z., Lu, K., Hofzumahaus, A., Fuchs, H., Bohn, B., Holland, F., Liu, Y., Rohrer, F., Shao, M., Sun, K., Wu, Y., Zeng, L., Zhang, Y., Zou, Q., Kiendler-Scharr, A., Wahner, A., and Zhang, Y.: Experimental budgets of OH, HO_2, and RO_2 radicals and implications for ozone formation in the Pearl River Delta in China 2014, Atmospheric Chemistry and Physics, 19, 7129–7150, https://doi.org/10.5194/acp-19-7129-2019, 2019.

Tanner, D. J., Jefferson, A., and Eisele, F. L.: Selected ion chemical ionization mass spectrometric measurement of OH, J. Geophys. Res., 102, 6415–6425, https://doi.org/10.1029/96JD03919, 1997.

Volz-Thomas, A., Pätz, H.-W., Houben, N., Konrad, S., and Mihelcic, D.: Inorganic trace gases and peroxy radicals during BERLIOZ at Pabstthum: An investigation of the photostationary state of NO_x and O_3, J. Geophys. Res., 108, 8248, https://doi.org/10.1029/2001JD001255, 2003a.

Volz-Thomas, A., Geiss, H., and Andreas, H.: Introduction to Special Section: Photochemistry Experiment in BERLIOZ, J. Geophys. Res., 108, 8252, https://doi.org/10.1029/2001JD002029, 2003b.

Wang, F., Hu, R., Chen, H., Xie, P., Wang, Y., Li, Z., Jin, H., Liu, J., and Liu, W.: Development of a field system for measurement of tropospheric OH radical using laser-induced fluorescence technique, Opt. Express, 27, A419, https://doi.org/10.1364/OE.27.00A419, 2019.

Wang, G., Iradukunda, Y., Shi, G., Sanga, P., Niu, X., and Wu, Z.: Hydroxyl, hydroperoxyl free radicals determination methods in atmosphere and troposphere, Journal of Environmental Sciences, 99, 324–335, https://doi.org/10.1016/j.jes.2020.06.038, 2021.

Whalley, L. K., Edwards, P. M., Furneaux, K. L., Goddard, A., Ingham, T., Evans, M. J., Stone, D., Hopkins, J. R., Jones, C. E., Karunaharan, A., Lee, J. D., Lewis, A. C., Monks, P. S., Moller, S. J., and Heard, D. E.: Quantifying the magnitude of a missing hydroxyl radical source in a tropical rainforest, Atmos. Chem. Phys., 11, 7223–7233, https://doi.org/10.5194/acp-11-7223-2011, 2011.

Whalley, L. K., Stone, D., Dunmore, R., Hamilton, J., Hopkins, J. R., Lee, J. D., Lewis, A. C., Williams, P., Kleffmann, J., Laufs, S., Woodward-Massey, R., and Heard, D. E.: Understanding in situ ozone production in the summertime through radical observations and modelling studies during the Clean air for London project (ClearfLo), Atmos. Chem. Phys., 18, 2547–2571, https://doi.org/10.5194/acp-

18-2547-2018, 2018.

Whalley, L. K., Slater, E. J., Woodward-Massey, R., Ye, C., Lee, J. D., Squires, F., Hopkins, J. R., Dunmore, R. E., Shaw, M., Hamilton, J. F., Lewis, A. C., Mehra, A., Worrall, S. D., Bacak, A., Bannan, T. J., Coe, H., Percival, C. J., Ouyang, B., Jones, R. L., Crilley, L. R., Kramer, L. J., Bloss, W. J., Vu, T., Kotthaus, S., Grimmond, S., Sun, Y., Xu, W., Yue, S., Ren, L., Acton, W. J. F., Hewitt, C. N., Wang, X., Fu, P., and Heard, D. E.: Evaluating the sensitivity of radical chemistry and ozone formation to ambient VOCs and NO_x in Beijing, Atmospheric Chemistry and Physics, 21, 2125–2147, https://doi.org/10.5194/acp-21-2125-2021, 2021.

Wolfe, G. M., Cantrell, C., Kim, S., Mauldin III, R. L., Karl, T., Harley, P., Turnipseed, A., Zheng, W., Flocke, F., Apel, E. C., Hornbrook, R. S., Hall, S. R., Ullmann, K., Henry, S. B., DiGangi, J. P., Boyle, E. S., Kaser, L., Schnitzhofer, R., Hansel, A., Graus, M., Nakashima, Y., Kajii, Y., Guenther, A., and Keutsch, F. N.: Missing peroxy radical sources within a summertime ponderosa pine forest, Atmos. Chem. Phys., 14, 4715–4732, https://doi.org/10.5194/acp-14-4715-2014, 2014.

Zhang, G., Hu, R., Xie, P., Lu, K., Lou, S., Liu, X., Li, X., Wang, F., Wang, Y., Yang, X., Cai, H., Wang, Y., and Liu, W.: Intercomparison of OH radical measurement in a complex atmosphere in Chengdu, China, Science of The Total Environment, 838, 155924, https://doi.org/10.1016/j.scitotenv.2022.155924, 2022a.

Zhang, G., Hu, R., Xie, P., Lou, S., Wang, F., Wang, Y., Qin, M., Li, X., Liu, X., Wang, Y., and Liu, W.: Observation and simulation of HO_x radicals in an urban area in Shanghai, China, Science of The Total Environment, 810, 152275, https://doi.org/10.1016/j.scitotenv.2021.152275, 2022b.